# Disassociation for Electronic Health Record Privacy

Grigorios Loukides[a], John Liagouris[b], Aris Gkoulalas-Divanis[c], Manolis Terrovitis[d]

[a]*School of Computer Science and Informatics, Cardiff University, United Kingdom*
[b]*Department of Electrical and Computer Engineering, NTUA, Greece*
[c]*IBM Research – Ireland, Dublin, Ireland*
[d]*IMIS, Research Center Athena, Greece*

**Abstract**

The dissemination of Electronic Health Record (EHR) data, beyond the originating healthcare institutions, can enable large-scale, low-cost medical studies that have the potential to improve public health. Thus, funding bodies, such as the National Institutes of Health (NIH) in the U.S., encourage or require the dissemination of EHR data, and a growing number of innovative medical investigations are being performed using such data. However, simply disseminating EHR data, after removing identifying information, may risk privacy, as patients can still be linked with their record, based on diagnosis codes. This paper proposes the first approach that prevents this type of data linkage using *disassociation*, an operation that transforms records by splitting them into carefully selected subsets. Our approach preserves privacy with significantly lower data utility loss than existing methods and does not require data owners to specify diagnosis codes that may lead to identity disclosure, as these methods do. Consequently, it can be employed when data need to be shared broadly and be used in studies, beyond the intended

*Email addresses:* g.loukides@cs.cf.ac.uk (Grigorios Loukides), liagos@dblab.ece.ntua.gr (John Liagouris), arisdiva@ie.ibm.com (Aris Gkoulalas-Divanis), mter@imis.athena-innovation.gr (Manolis Terrovitis)

ones. Through extensive experiments using EHR data, we demonstrate that our method can construct data that are highly useful for supporting various types of clinical case count studies and general medical analysis tasks.
*Keywords:* privacy, electronic health records, disassociation, diagnosis codes

## 1. Introduction

Healthcare data are increasingly collected in various forms, including Electronic Health Records (EHR), medical imaging databases, disease registries, and clinical trials. Disseminating these data has the potential of offering better healthcare quality at lower costs, while improving public health. For instance, large amounts of healthcare data are becoming publicly accessible at no cost, through *open data* platforms [4], in an attempt to promote accountability, entrepreneurship, and economic growth ($100 billion are estimated to be generated annually across the US health-care system [11]). At the same time, sharing EHR data can greatly reduce research costs (e.g., there is no need for recruiting patients) and allow large-scale, complex medical studies. Thus, the National Institutes of Health (NIH) calls for increasing the reuse of EHR data [7], and several medical analytic tasks, ranging from building predictive data mining models [8] to genomic studies [14], are being performed using such data.

Sharing EHR data is highly beneficial but must be performed in a way that preserves patient and institutional privacy. In fact, there are several data sharing policies and regulations that govern the sharing of patient-specific data, such as the HIPAA privacy rule [46], in the U.S., the Anonymization Code [6], in the U.K., and the Data Protection Directive [3], in the European Union. In addition, funding bodies emphasize the need for privacy-preserving healthcare data

sharing. For instance, the NIH requires data involved in all NIH-funded Genome-Wide Association Studies (GWAS) to be deposited into a biorepository, for broad dissemination [44], while safeguarding privacy [1]. Alarmingly, however, a large number of privacy breaches, related to healthcare data, still occur. For example, 627 privacy breaches, which affect more than 500 and up to 4.9M individuals each, are reported from 2010 to July 2013 by the U.S. Department of Health & Human Services [15].

One of the main privacy threats when sharing EHR data is *identity disclosure* (also referred to as *re-identification*), which involves the association of an identified patient with their record in the published data. Identity disclosure may occur even when data are *de-identified* (i.e., they are devoid of identifying information). This is because publicly available datasets, such as voter registration lists, contain identifying information and can be linked to published datasets, based on potentially identifying information, such as demographics [51], diagnosis codes [33], and lab results [9]. The focus of our work is on diagnosis codes, because: (i) they pose a high level of re-identification risk [33], and (ii) ensuring that diagnosis codes are shared in a privacy-preserving way, is challenging, due to their characteristics [54, 25, 28]. For example, more than 96% of 2700 patient records that are involved in an NIH-funded GWAS were shown to be uniquely re-identifiable, based on diagnosis codes, and, applying popular privacy-preserving methods, distorts the published data to the point that they lose their clinical utility [33].

To see how identity disclosure may occur, consider the de-identified data in Fig. 1. In these data, each record corresponds to a distinct patient and contains the set of diagnosis codes that this patient is associated with. The description of the diagnosis codes in Fig. 1 is shown in Fig. 2. An attacker, who knows that a

patient is diagnosed with *Bipolar I disorder, single manic episode, mild* (denoted with the code $296.01$) and *Closed dislocation of finger, unspecified part* (denoted with $834.0$), can associate an identified patient with the first record, denoted with $r_1$, in the data of Fig. 1, as the set of codes $\{296.01, 834.0\}$ appears in no other record. Notice that, in this work, we consider ICD-9 codes[1], following [35, 34]. However, our approach can be applied to other standardized codes, such as Common Procedure Terminology (CPT) codes.

| ID | Records |
|---|---|
| $r_1$ | {296.00, 296.01, 296.02, 834.0, 944.01} |
| $r_2$ | {296.00, 296.02, 296.01, 401.0, 944.01, 692.71, 695.10} |
| $r_3$ | {296.00, 296.02, 692.71, 834.0, 695.10} |
| $r_4$ | {296.00, 296.01, 692.71, 401.0} |
| $r_5$ | {296.00, 296.01, 296.02, 692.71, 695.10} |
| $r_6$ | {296.03, 295.04, 404.00, 480.1} |
| $r_7$ | {294.10, 296.03, 834.0, 944.01} |
| $r_8$ | {294.10, 295.04, 296.03, 480.1} |
| $r_9$ | {294.10, 295.04, 404.00} |
| $r_{10}$ | {294.10, 295.04, 296.03, 834.0, 944.01} |

Figure 1: Original dataset $D$.

| Diagnosis code | Description |
|---|---|
| 294.10 | Dementia in conditions classified elsewhere without behavioral disturbance |
| 295.04 | Simple type schizophrenia, chronic with acute exacerbation |
| 296.00 | Bipolar I disorder, single manic episode, unspecified |
| 296.01 | Bipolar I disorder, single manic episode, mild |
| 296.02 | Bipolar I disorder, single manic episode, moderate |
| 296.03 | Bipolar I disorder, single manic episode, severe, without mention of psychotic behavior |
| 401.0 | Malignant essential hypertension |
| 404.00 | Hypertensive heart and chronic kidney disease, malignant, without heart failure and with chronic kidney disease stage I through stage IV, or unspecified |
| 480.1 | Pneumonia due to respiratory syncytial virus |
| 692.71 | Sunburn |
| 695.10 | Erythema multiforme, unspecified |
| 834.0 | Closed dislocation of finger, unspecified part |
| 944.01 | Burn of unspecified degree of single digit (finger (nail) other than thumb |

Figure 2: Diagnosis codes in $D$ and their description.

[1] http://www.cdc.gov/nchs/data/icd9/icdguide10.pdf

### *1.1. Motivation*

Preventing identity disclosure based on diagnosis codes is possible by applying the methods proposed in [35, 34]. Both methods transform diagnosis codes to ensure that the probability of performing identity disclosure, based on *specified* sets of diagnosis codes, will not exceed a data-owner specified parameter $k$. Data transformation is performed using *generalization* (i.e., by replacing diagnosis codes with more general, but semantically consistent, ones) and *suppression* (i.e., by deleting diagnosis codes). Furthermore, both methods aim at transforming data in a way that does not affect the findings of biomedical analysis tasks that the data are intended for. These tasks are specified by data owners and used to control the potential ways diagnosis codes are generalized and/or suppressed. For example, applying the CBA algorithm [34], which outperforms the method in [35] in terms of preserving data utility, to the data in Fig. 1, produces the data in Fig. 3a. In this example, CBA was applied using $k = 3$ and with the goal of (i) thwarting identity disclosure, based on all sets of 2 diagnosis codes, and (ii) preserving the findings of studies $u_1$ to $u_5$ in Fig. 3b, which require counting the number of patients diagnosed with any combination of codes in them. Observe that the codes 294.10, 295.04, and 296.00 to 296.03 are generalized to $(294.10, 295.04, 296.00, 296.01, 296.02, 296.03)$, which is interpreted as any non-empty subset of these codes, and that 7 out of 13 distinct codes are suppressed. The result of CBA thwarts identity disclosure (i.e., all combinations of 2 diagnosis codes appear at least 3 times in Fig. 3a) and allows performing $u_1$ and $u_3$ accurately. To see why this is the case, consider $u_3$, for example. Note that $4$ patients are associated with a combination of the codes $\{401.0, 404.00\}$ in $u_3$, in both Fig. 1 and in Fig. 3a). However, the studies $u_2$, $u_4$, and $u_5$ can no longer be performed

accurately, as some of their associated diagnosis codes have been suppressed.

| ID | Records |
|---|---|
| $r_1$ | (294.10, 295.04, 296.00, 296.01, 296.02, 296.03), *834.0, 944.01* |
| $r_2$ | (294.10, 295.04, 296.00, 296.01, 296.02, 296.03), (401.0, 404.00), *944.01, 692.71, 695.10* |
| $r_3$ | (294.10, 295.04, 296.00, 296.01, 296.02, 296.03), *692.71, 834.0, 695.10* |
| $r_4$ | (294.10, 295.04, 296.00, 296.01, 296.02, 296.03), (401.0, 404.00), *692.71* |
| $r_5$ | (294.10, 295.04, 296.00, 296.01, 296.02, 296.03), *692.71, 695.10* |
| $r_6$ | (294.10, 295.04, 296.00, 296.01, 296.02, 296.03), (401.0, 404.00), *480.1* |
| $r_7$ | (294.10, 295.04, 296.00, 296.01, 296.02, 296.03), *834.0, 944.01* |
| $r_8$ | (294.10, 295.04, 296.00, 296.01, 296.02, 296.03), *480.1* |
| $r_9$ | (294.10, 295.04, 296.00, 296.01, 296.02, 296.03), (401.0, 404.00) |
| $r_{10}$ | (294.10, 295.04, 296.00, 296.01, 296.02, 296.03), *834.0, 944.01* |

(a) Anonymized dataset $D^A$ produced by *CBA* (suppressed codes appear in gray).

| ID | Utility constraints |
|---|---|
| $u_1$ | {294.10, 295.04, 296.00, 296.01, 296.02, 296.03} |
| $u_2$ | {692.71, 695.10} |
| $u_3$ | {401.0, 404.00} |
| $u_4$ | {480.1} |
| $u_5$ | {834.0, 944.01} |

(b) Utility constraints.

Figure 3: *CBA* example.

In fact, the methods in [35, 34] assume a setting in which data owners possess domain expertise that allows them to specify: (i) sets of diagnosis codes that lead to identity disclosure, and (ii) sets of diagnosis codes that model analytic tasks that the published data are intended for. The ability of the published data to support these tasks is a strong requirement, and suppression is used when this requirement cannot be satisfied[2]. As can be seen in Fig. 3a, the fact that $u_2 = \{692.71, 695.10\}$ was not satisfied led CBA to suppress both 692.71 and 695.10. The setting considered in [35, 34] can model some real data sharing scenarios, such as the sharing of data between collaborating researchers, who perform specific analytic tasks [35].

However, it is important to consider a different setting, where data are shared more broadly and may be used for studies beyond those that are specified by

[2]Due to the computational complexity of the problem, no guarantees that these requirements will be satisfied are provided by the methods in [35, 34].

data owners. This setting becomes increasingly common, as databanks (e.g.,[2, 5]) host a wide range of patient-specific data and grow in size and popularity. Addressing this setting calls for developing methods that offer strong privacy and permit the publishing of data that remain useful, for analytic tasks that cannot be predetermined, in addition to any intended ones. In fact, the aforementioned methods [35, 34] are not suitable for this setting, because their application would cause excessive loss of data utility, as it will become clear later.

### *1.2. Contributions*

In this paper, we propose the first approach for the privacy-preserving sharing of diagnosis codes under this new setting. Our approach allows data owners to share data that prevent identity disclosure, and does not incur excessive information loss or harm the usefulness of data in medical analysis. This work makes the following specific contributions.

First, we develop an effective algorithm that prevents identity disclosure, based on all sets of $m$ or fewer diagnosis codes, by limiting its probability to $\frac{1}{k}$, where $k$ and $m$ are data-owner specified parameters. To achieve this, the algorithm transforms data using *disassociation*, an operation that splits the records into carefully constructed subrecords, containing original (i.e., non-transformed) diagnosis codes. Thus, strong privacy requirements can be specified, without knowledge of potentially identifying diagnosis codes, and they can be enforced with low information loss. In addition, analytic tasks that published data are intended for can still be performed highly accurately. For instance, as can be seen in Fig. 4, applying our algorithm to the data in Fig. 1, using $k = 3$ and $m = 2$, achieves the same privacy, but significantly better data utility, than CBA, whose result is shown in Fig. 3a. This is because, in contrast to CBA, our algorithm does not suppress

diagnosis codes and retains the exact counts of 8 out of 13 codes (i.e., those in $u_1$ and $u_3$). Moreover, our algorithm is able to preserve the findings of the first two studies in Fig. 3b.

Second, we experimentally demonstrate that our approach preserves data utility significantly better than the state-of-the-art method [34]. Specifically, when applied to a large EHR dataset [8], our approach allows up to 16 times more accurate query answering and generates data that are highly useful for supporting various types of clinical case count studies and general medical analysis tasks.

### *1.3. Paper organization*

The remainder of the paper is organized as follows. Section 2 reviews related work and Section 3 presents the concepts that are necessary to introduce our method and formulate the problem we consider. In Sections 4 and 6, we discuss and experimentally evaluate our algorithm, respectively. Subsequently, we explain how our approach can be extended to deal with different types of medical data and privacy requirements in Section 7. Last, Section 8 concludes the paper.

Cluster $P_1$ $|P_1| = 5$

| | **Record chunks** | | **Item chunk** |
|---|---|---|---|
| | $C_1$ | $C_2$ | $C_T$ |
| $r_1$ | {296.00, 296.01, 296.02} | | |
| $r_2$ | {296.00, 296.01, 296.02} | {692.71, 695.10} | 834.0, 401.0, |
| $r_3$ | {296.00, 296.02} | {692.71, 695.10} | 944.01 |
| $r_4$ | {296.00, 296.01} | {692.71} | |
| $r_5$ | {296.00, 296.01, 296.02} | {692.71, 695.10} | |

Cluster $P_2$ $|P_2| = 5$

| | **Record chunk** | **Item chunk** |
|---|---|---|
| | $C_1$ | $C_T$ |
| $r_6$ | {296.03, 295.04} | |
| $r_7$ | {294.10, 296.03} | 404.00, |
| $r_8$ | {294.10, 295.04, 296.03} | 480.1, 834.0, 944.01 |
| $r_9$ | {294.10, 295.04} | |
| $r_{10}$ | {294.10, 295.04, 296.03} | |

Figure 4: Anonymized dataset $D^A$ using our DISSASSOCIATION method. The dataset is comprised of two clusters, and each record is comprised of a number of subrecords, called *chunks*.

## 2. Related work

We focus on preventing identity disclosure in a *non-interactive data sharing scenario* that involves broad data dissemination to potentially unknown data recipients. This scenario has many benefits [23] and allows wider and more effective use of the shared data. However, the fact that data are disseminated beyond a small number of authorized recipients poses new privacy challenges, which cannot be addressed by access control [50] and encryption-based [47, 55, 22, 10] methods. We also assume that data must be shared at a patient level, which is crucial to enable clinical studies in several fields, such as those in epidemiology [42] and genetics [35].

The threat of identity disclosure in medical data publishing was firstly pointed out by Sweeney [49], and it has since attracted significant research interest [26, 19, 41, 17, 20, 18, 43]. Although other threats have been considered [40, 39, 56, 38], "*all the publicly known examples of re-identification of personal information have involved identity disclosure*" [18]. The majority of works focus on preventing identity disclosure via relational data (i.e., data in which a patient is associated with a fixed, and typically small number of attributes), which naturally model patient demographics. Attacks based on demographics can be thwarted using $k$-anonymity [49, 51], which requires each record in the shared dataset to have the same values with at least $k$-1 other records in potentially identifying attributes (also known as *quasi-identifiers*). To enforce $k$-anonymity, *suppression* [49, 51], which deletes certain values prior to data sharing, or *generalization* [49, 51, 30], which replaces values with more general, but semantically consistent values, can be applied. Different from this line of research, we consider data containing diagnosis codes, which require different handling than relational data, and apply

disassociation, which generally incurs lower information loss than generalization and suppression.

Anonymizing diagnosis codes can be achieved by modeling them using a *transaction* attribute and enforcing a privacy model for transaction data [36, 38, 28, 54, 58, 52, 37]. The value in a transaction attribute is a set of *items* (itemset), which, in our case, corresponds to a patient's diagnosis codes. In [28], He et al. proposed *complete* $k$*-anonymity* to prevent an attacker from linking an individual to fewer than $k$ records in the published dataset, even when the attacker knows all items of a transaction. To enforce this principle, He et al. [28] proposed a generalization-based algorithm, called *Partition*. Terrovitis et al. [28] argued that attackers are unlikely to know all items of an individual and proposed $k^m$-anonymity to guard against attackers who know up to $m$ items. The authors of [28] designed the Apriori algorithm, which operates in a bottom-up fashion, beginning with 1-itemsets (items) and subsequently considering incrementally larger itemsets. In each iteration, Apriori enforces $k^m$-anonymity using the full-subtree, global generalization model [57]. Xu et al. [58] proposed a privacy model that treats (*public*) items similarly to $k^m$-anonymity and a suppression-based algorithm to enforce it. The algorithm of [58] discovers all unprotected itemsets of minimal size and protects them by iteratively suppressing the item contained in the greatest number of those itemsets.

Loukides et al. [35] showed that the algorithms proposed in [28, 54, 58] are not suited to anonymizing diagnosis codes. This is because, they explore a small number of possible ways to anonymize diagnosis codes, and they are inadequate to generate data that support biomedical analysis tasks. In response, they proposed two algorithms for anonymizing diagnosis codes [35, 34]. The first of these algo-

rithms, called *Utility-Guided Anonymization of Clinical Profiles* (UGACLIP) applies generalization to sets of diagnosis codes that may lead to identity disclosure in a way that: (i) limits the probability of identity disclosure, based on these sets of codes, (ii) aims at preserving the intended analysis tasks, which are modeled as associations between diagnosis codes using *utility constraints*, and (iii) incurs a minimal amount of information loss. The sets of potentially identifying diagnosis codes, as well as utility constraints, are specified by data owners and given as input to UGACLIP. However, UGACLIP may overdistort diagnosis codes that are not contained in the specified associations, which limits the ability to use the generated data in tasks that are not related to the specified associations [34]. To address these limitations, an algorithm, called *Clustering-Based Anonymizer* (CBA) was proposed in [34]. CBA uses the same privacy and utility model as UGACLIP but employs a more effective heuristic both in terms of supporting the intended medical analysis tasks and in terms of incurring a small amount of information loss. As discussed in Introduction, our approach is developed for a different data sharing scenario than that of [35, 34], and it applies a different privacy model and data transformation technique.

Another privacy model, called *differential privacy* [16], has attracted significant attention [45, 29, 21] and has recently been applied to medical data [24]. Differential privacy ensures that the outcome of a calculation is insensitive to any particular record in the dataset. This offers privacy, because the inferences that can be made about an individual will be (approximately) independent of whether any individuals record is contained in the dataset or not. Differential privacy makes no assumptions about an attacker's background knowledge, unlike $k^m$-anonymity, although its enforcement does not guarantee the prevention of all attacks [12].

However, differential privacy allows either noisy answers to a limited number of queries, or noisy summary statistics to be released, and there are a number of limitations regarding its application on healthcare data [13]. In addition, differentially private data may be of much lower utility compared to $k^m$-anonymous data produced by disassociation, as shown in [53].

## 3. Background

In the previous sections, we highlighted how a patient can be identified by simply tracing records that contain unique combinations of diagnosis codes. Here, we present a concrete attack model and an effective data transformation operation, called *disassociation*. Disassociation can be used to guarantee patient privacy with respect to this model, while incurring minimal data utility loss. To quantify the loss of data utility caused by disassociation, we also discuss two measures that capture different requirements of medical data applications.

### *3.1. Attack Model and Privacy Guarantee*

We assume a dataset $D$ of records (transactions), each of which contains a set of diagnosis codes (items) from a finite domain $T$. The number of records in $D$ is denoted with $|D|$. Each record in $D$ refers to a different patient and contains the set of all diagnosis codes associated with them. An example of a dataset is shown in Fig. 1. Each record in this dataset contains some diagnosis codes, and the domain of diagnosis codes is shown in Fig. 2. In contrast to the traditional attack models for relational data [40, 32], we do not distinguish between sensitive (unknown to the attacker) and non-sensitive items in a record. Instead, we assume that any item is a potential quasi-identifier and, hence, it may lead to identity disclosure. Besides the dataset $D$ we also assume a set of utility constraints $U$

[35], also referred to as *utility policy*. As discussed in Section 2, utility constraints model associations between diagnosis codes that anonymized data are intended for. Each utility constraint $u$ in $U$ is a set of items from $T$, and all constraints in $U$ are disjoint. Fig. 3b illustrates an example of a set of utility constraints.

We now explain the attack model considered in this work. In this model, an attacker knows up to $m$ items of a record $r$ in $D$, where $m \geq 1$. The case of attackers with no background knowledge (i.e., $m = 0$) is trivial, and it is easy to see that the results of our theoretical analysis are applicable to this setting as well. Note that, different from the methods in [35, 34], the items that may be exploited by attackers are considered unknown to data owners. Also, there may be multiple attackers, each of which knows a (not necessarily distinct) set of up to $m$ items of a record $r$. Other attacks and the ability of our method to thwart them are discussed in Section 7.

Based on their knowledge, an attacker can associate the identified patient with their record $r$, breaching privacy. To thwart this threat, our work employs the privacy model of $k^m$*-anonymity* [54]. $k^m$-anonymity is a conditional form of $k$-anonymity, which ensures that an attacker with partial knowledge of a record $r$, as explained above, will not be able to distinguish $r$ from $k-1$ other records in the published dataset. In other words, the probability that the attacker performs identity disclosure is upperbounded by $\frac{1}{k}$. More formally:

**Definition 1.** *An anonymized dataset $D^A$ is $k^m$-anonymous if no attacker with background knowledge of up to $m$ items of a record $r$ in $D^A$ can use these items to identify fewer than $k$ candidate records in $D^A$.*

For the original dataset $D$ and its anonymized counterpart $D^A$, we define two transformations $\mathcal{A}$ and $\mathcal{I}$. The anonymization transformation $\mathcal{A}$ takes as input

a dataset $D$ and produces an anonymized dataset $D^A$. The inverse transformation $\mathcal{I}$ takes as input the anonymized dataset $D^A$ and outputs all possible (non-anonymized) datasets that could produce $D^A$, i.e., $\mathcal{I}(D^A) = \{D' \mid D^A = \mathcal{A}(D)\}$. Obviously, the original dataset $D$ is one of the datasets in $\mathcal{I}(\mathcal{A}(D))$. To achieve $k^m$-anonymity (Definition 1) in our setting, we enforce the following privacy guarantee (from [53]).

**Guarantee 1.** *Consider an anonymized dataset $D^A$ and a set $\mathcal{S}$ of up to $m$ items. Applying $\mathcal{I}(D^A)$, will always produce at least one dataset $D' \in \mathcal{I}(D^A)$ for which there are at least $k$ records that contain all items in $\mathcal{S}$.*

Intuitively, an attacker, who knows any set $\mathcal{S}$ of up to $m$ diagnosis codes about a patient, will have to consider at least $k$ candidate records in a possible original dataset. We provide a concrete example to illustrate this in the next subsection.

### *3.2. Overview of the disassociation transformation strategy*

In this section, we present disassociation, a data transformation strategy that partitions the records in the original dataset $D$ into subrecords, following the basic principles of the strategy presented in [53]. The goal of our strategy is to "hide" combinations of diagnosis codes that appear few times in $D$, by scattering them in the subrecords of the published dataset. The particular merit of disassociation is that it preserves all original diagnosis codes in the published dataset, in contrast to generalization and suppression. This is important to preserve data utility in various medical analysis tasks that cannot be predetermined, as explained in the introduction and will be verified experimentally.

To illustrate the main idea of disassociation, we use Fig. 4, which shows a disassociated dataset produced from the original dataset $D$ of Fig. 1. Observe

that the dataset in Fig. 4 is divided into two *clusters*, $P_1$ and $P_2$, which contain the records $r_1{-}r_5$ and $r_6{-}r_{10}$, respectively. Furthermore, the diagnosis codes in a cluster are divided into subsets, and each record in the cluster is split into subrecords according to these subsets. For example, the diagnosis codes in $P_1$ are divided into subsets $T_1 =\{296.00, 296.01, 296.02\}$, $T_2 =\{692.71, 695.10\}$, and $T_T =\{834.0, 401.0, 944.01\}$, according to which $r_1$ is split into three subrecords; $\{296.00, 296.01, 296.02\}$, an empty subrecord $\{\}$, and $\{834.0, 944.01\}$. The collection of all subrecords of different records that correspond to the same subset of diagnosis codes is called a *chunk*. For instance, the subrecord $\{296.00, 296.01, 296.02\}$ of $r_1$ goes into chunk $C_1$, the empty subrecord goes into chunk $C_2$, and the subrecord $\{834.0, 944.01\}$ goes into chunk $C_T$. In contrast to $C_1$ and $C_2$ which are *record chunks*, $C_T$ is a special, *item chunk*, containing a single set of diagnosis codes. In our example, $C_T$ contains the set $\{834.0, 401.0, 944.01\}$, which represents the subrecords from all $r_1{-}r_5$ containing these codes. Thus, the number of times each diagnosis code in $C_T$ appears in the original dataset is completely hidden from the attacker, who can only assume that this number ranges from 1 to $|P_i|$, where $|P_i|$ is the number of records in $P_i$.

In addition, the order of the subrecords that fall into a chunk is randomized, which implies that the association between subrecords in different chunks is hidden from the attacker. In fact, the original dataset $D$ may contain any record that could be *reconstructed* by a combination of subrecords from the different chunks plus *any subset of diagnosis codes* from $C_T$. For example, $\{296.00, 296.01, 834.0, 944.01\}$ in Fig. 5 is a reconstructed record, which is created by taking $\{296.00, 296.01\}$ from $C_1$, the empty subrecord $\{\}$ from $C_2$, and $\{834.0, 944.01\}$ from $C_T$. Observe that this record does not appear in the original dataset of Fig. 1.

The disassociated dataset $D^A$ amounts to the set of all possible original datasets $\mathcal{I}(D^A)$ (see Guarantee 1). In other words, the original dataset $D$ is *hidden*, among all possible datasets that can be reconstructed from $D^A$. A dataset, which is reconstructed from the disassociated dataset in Fig. 4, is shown in Fig. 5. Note that reconstructed datasets can be greatly useful to data analysts, because (i) they have similar statistical properties to the original dataset from which they are produced, and (ii) they can be analyzed directly, using off-the-shelf tools (e.g., SPSS), in contrast to generalized datasets that require special handling (e.g., interpreting a generalized code as an original diagnosis code, with a certain probability).

As an example, consider the dataset in Fig. 4, which satisfies Guarantee 1, for $k = 3$ and $m = 2$. Observe that an attacker, who knows up to $m = 2$ codes from a record $r$ of the original dataset in Fig. 1, must consider a reconstructed dataset that has at least 3 records containing the codes known to them. We emphasize that each of these codes can appear in any chunk of a cluster in $D^A$, including the item chunk. For instance, an attacker, who knows that the record of a patient contains 296.01 and 834.0, must consider the dataset in Fig. 5. In this dataset, the combination of these codes appears in the records $r_1$, $r_2$, and $r_3$.

| ID | Records |
|---|---|
| $r_1$ | {296.00, 296.01, 834.0, 944.01} |
| $r_2$ | {296.02, 296.01, 692.71, 834.0} |
| $r_3$ | {296.00, 296.01, 296.02, 692.71, 695.10, 834.0} |
| $r_4$ | {296.00, 296.02, 692.71, 695.10} |
| $r_5$ | {296.00, 296.01, 296.02, 692.71, 695.10, 401.0} |
| $r_6$ | {296.02, 295.04, 480.1} |
| $r_7$ | {294.10, 296.02, 404.00, 834.0, 944.01} |
| $r_8$ | {294.10, 295.04, 296.02, 480.1, 834.0} |
| $r_9$ | {294.10, 295.04, 404.00, 834.0} |
| $r_{10}$ | {294.10, 295.04, 296.02, 834.0, 944.01} |

Figure 5: A possible dataset $D'$ reconstructed from $D^A$ of Figure 4.

### *3.3. Measuring Data Utility*

Different datasets that can be produced by an original dataset, using disassociation, do not offer the same utility. In addition, most existing measures for anonymized data using generalization and/or suppression, such as those proposed in [54, 58, 35, 34], are not applicable to disassociated datasets. Therefore, we measure data utility using the accuracy of: (i) answering COUNT queries on disassociated data, and (ii) estimating the number of records that are associated with any set of diagnosis codes in a utility constraint (i.e., *matched* to the constraint). The first way to measure data utility considers a scenario in which data recipients issue queries to perform *case counting* (i.e., discover the number of patients diagnosed with a set of one or more diagnosis codes, using COUNT queries). Alike other transformation strategies, disassociation may degrade the accuracy of answering COUNT queries [35, 53]. Thus, a utility measure must capture how accurately such queries can be answered using disassociated data. The second way to quantify data utility considers a scenario in which various analytic tasks, simulated through different utility policies, are performed by data recipients. To the best of our knowledge, there are no measures that can capture data utility in this scenario.

To quantify the accuracy of answering a workload of COUNT queries on disassociated data, we use the *Average Relative Error* (ARE) measure, a standard data utility indicator [35, 34, 53], which reflects the average number of transactions that are retrieved incorrectly as part of query answers. The following definition explains how ARE can be computed.

**Definition 2.** *Let $\mathcal{W}$ be a workload of COUNT queries $q_1, ..., q_n$, and $C_A$ and $C_O$ be functions which count the number of records answering a query $q_i$, $i \in [1, n]$*

*on the anonymized dataset $D'$ and on the original dataset $D$, respectively. The ARE measure for $\mathcal{W}$ is computed as*

$$ARE(\mathcal{W}) = avg_{\forall i \in [1,n]} \frac{|C_A(q_i) - C_O(q_i)|}{C_O(q_i)}$$

Thus, ARE is computed as the mean error of answering all queries in the query workload $\mathcal{W}$. Clearly, a zero ARE implies that the anonymized dataset $D'$ are as useful as the original dataset in answering the queries in $\mathcal{W}$, and low scores in ARE are preferred.

To capture data utility in the presence of specified utility policies, we propose a new measure, called *Matching Relative Error* (MRE). The computation of MRE is illustrated in the following definition.

**Definition 3.** *Let $u$ be a utility constraint in $U$, and $M_A$ and $M_O$ be functions, which return the number of records that match $u$ in the anonymized dataset $D'$ and in the original dataset $D$, respectively. The MRE for $u$ is computed as*

$$MRE(u) = \frac{M_O(u) - M_A(u)}{M_O(u)}$$

Thus, a zero MRE implies that an anonymized dataset can support $u$ as well as the original dataset does, and MRE scores close to zero are preferred. For clarity, we report MRE as a percentage (i.e., the *percent error*). For example, an MRE in the interval $[-5\%, 5\%]$ implies that the number of transactions that match the utility constraint in the anonymized dataset is no more than $5\%$ different (larger

or smaller) than the corresponding number in the original dataset.

It is easy to see that ARE and MRE are applicable to several different workloads and utility constraints, respectively. For instance, in our experiments (Section 6), we used workloads containing sets of diagnosis codes that a certain percentage of all patients have, and utility constraints that model semantic relationships between diagnosis codes. Also, Definitions 2 and 3 refer to an anonymized dataset $D'$, without restricting the data transformation strategy applied to produce it. For instance, $D'$ can be a reconstructed dataset, such as the dataset in Fig. 5, or a generalized dataset, such as the dataset in Fig. 3a.

## 4. Disassociation algorithm

This section presents our disassociation-based algorithm for anonymizing diagnosis codes, which is referred to as DISASSOCIATION. This algorithm performs three operations: (i) *horizontal partitioning*, (ii) *vertical partitioning*, and (iii) *refining*. Horizontal partitioning brings together similar records with respect to diagnosis codes into clusters. As will be explained, performing this operation is important to preserve privacy with low utility loss. Subsequently, the algorithm performs vertical partitioning. This operation, which is the heart of our method, disassociates combinations of diagnosis codes that require protection and creates chunks. DISASSOCIATION differs from the method of [53] in that it aims at producing data that satisfy utility constraints and hence remain useful in medical analysis. Specifically, the horizontal and vertical partitioning phases in our algorithm treat codes that are contained in utility constraints as first-class citizens, so that they are preserved in the published dataset to the largest possible extent. Last, our algorithm performs the refining operation, to further reduce information

loss and improve the utility of the disassociated data, A high-level pseudocode of DISASSOCIATION is given in Fig. 6. In addition, Fig. 7 summarizes the notation used in our algorithm and in the algorithms that perform its operations.

**Algorithm**: DISASSOCIATION
**Input** : Original dataset $D$,
parameters $k$ and $m$
**Output** : Disassociated dataset $D^A$

1 Split $D$ into disjoint clusters by applying Algorithm HORPART;
2 **for** *every cluster* $P$ *produced* **do**
3 Split $P$ vertically into chunks by applying Algorithm VERPART;
4 Refine clusters;
5 **return** $D^A$;

Figure 6: DISASSOCIATION algorithm.

| Symbol | Explanation |
|---|---|
| $D$, $D^A$ | Original, anonymized dataset |
| $T$ | The set of all diagnosis codes in $D$ |
| $U$ | Set of utility constraints |
| $T_U$ | The set of all diagnosis codes in $U$ |
| $s(\mathsf{a})$ | Support of diagnosis code $\mathsf{a}$ |
| $P, P_1 \ldots$ | Clusters |
| $T^P$ | Domain of cluster |
| $C, C_1, \ldots$ | Record chunks |
| $T_1, T_2, \ldots$ | Domain of record chunk |
| $C_T$ | Item chunk |
| $T_T$ | Domain of item chunk |

Figure 7: Notation used in our DISASSOCIATION algorithm and in the algorithms HORPART and VERPART.

In the following, we present the details of the horizontal partitioning, vertical partitioning, and refining operations of our algorithm.

**Horizontal partitioning.** This operation groups records of the original dataset $D$ into disjoint *clusters*, according to the similarity of diagnosis codes. For instance, cluster $P_1$ is formed by records $r_1{-}r_5$, which have many codes in common, as

can be seen in Fig. 4. The creation of clusters is performed with a light-weight, but very effective heuristic, called HORPART. The pseudocode of HORPART is provided in Fig. 8. This heuristic aims at creating coherent clusters, whose records will require the least possible disassociation, during vertical partitioning.

To achieve this, the key idea is to split the dataset into two parts, $D_1$ and $D_2$, according to: (i) the *support* of diagnosis codes in $D$ (the support of a diagnosis code $\mathsf{a}$, denoted with $s(\mathsf{a})$, is the number of records in $D$ in which $\mathsf{a}$ appears), and (ii) the participation of diagnosis codes in the utility policy $U$. At each step, $D_1$ contains all records with the diagnosis code $\mathsf{a}$, whereas $D_2$ contains the remaining records. This procedure is applied recursively, to each of the constructed parts, until they are small enough to become clusters. Diagnosis codes that have been previously used for partitioning are recorded in a set $ignore$ and are not used again.

In each recursive call, Algorithm HORPART selects a diagnosis code $\mathsf{a}$, in lines 3-10. In the first call, $\mathsf{a}$ is selected as the most frequent code (i.e., the code with the largest support), which is contained in a utility constraint. At each subsequent call, $\mathsf{a}$ is selected as the most frequent code, among the codes contained in $u$ (i.e., the utility constraint with the code chosen in the previous call) (line 4). When all diagnosis codes in $u$ have been considered, $\mathsf{a}$ is selected as the most frequent code in the set $\{T-ignore\}$, which is also contained in a utility constraint (line 6). Of course, if no diagnosis code is contained in a utility constraint, we simply select $\mathsf{a}$ as the most frequent diagnosis code (line 9).

Horizontal partitioning reduces the task of anonymizing the original dataset to the anonymization of small and independent clusters. This way the privacy guarantee can be achieved more efficiently, since the disassociation process is restricted in the scope of each created cluster, as described below.

**Algorithm**: HORPART
**Input** : Dataset $D$,
set of diagnosis codes $ignore$ (initially empty),
a utility constraint $u \in U$ (initially empty)
**Output** : A HORizontal PARTitioning of $D$, i.e., a set of clusters
**Param.** : The maximum cluster size $maxClusterSize$

Let $T$ be the set of diagnosis codes in $D$, and $T_U$ be the set of diagnosis codes appearing in the utility constraints of $U$;
**if** $|D| < maxClusterSize$ **then return** $\{\!\{D\}\!\}$;
**if** $\{T - ignore\} \bigcap u \neq \{\}$ **then**
    Find the most frequent diagnosis code a in $\{T - ignore\} \bigcap u$;
**else if** $\{T - ignore\} \bigcap T_U \neq \{\}$ **then**
    Find the most frequent diagnosis code a in $\{T - ignore\} \bigcap T_U$;
    $u \leftarrow$ the constraint a belongs to;
**else**
    Find the most frequent diagnosis code a in $\{T - ignore\}$;
    $u \leftarrow \{\}$;
$D_1 \leftarrow$ the set of all records of $D$ that have a;
$D_2 \leftarrow D - D_1$;
**return** HORPART$(D_1, ignore \cup \mathsf{a}, u) \cup$HORPART$(D_2, ignore, \{\})$

Figure 8: HORPART algorithm.

**Vertical partitioning.** This operation partitions the clusters into chunks, using a greedy heuristic that is applied to each cluster independently. The intuition behind the operation of this heuristic, called VERPART, is twofold. First, the algorithm tries to distribute infrequent combinations of codes into different chunks to preserve privacy, as in [53]. Second, it aims at satisfying the utility constraints, in which the diagnosis codes in the cluster are contained. To achieve this, the algorithm attempts to create record chunks, which contain as many diagnosis codes from the same utility constraint as possible. Clearly, creating a record chunk that contains all the diagnosis codes of one or more utility constraints is beneficial, as tasks involving these codes (e.g., clinical case count studies) can be performed as

accurately as in the original dataset.

**Algorithm**: VERPART
**Input** : A cluster $P$, parameters $k$ and $m$
**Output** : A $k^m$-anonymous VERtical PARTitioning of $P$

Let $T^P$ be the set of diagnosis codes of $P$;
**for** *every diagnosis code* $t \in T^P$ **do**
    Compute the support $s(t)$;
Move all diagnosis codes with $s(t) < k$ from $T_P$ into $T_T$; // $T_T$ is finalized
Identify the groups of diagnosis codes in $T^P$ that belong to the same utility constraint of $U$, sort the diagnosis codes of each group in decreasing $s(t)$, and then sort the groups in decreasing $s(t)$ of their first diagnosis code;
$i \leftarrow 0$;
$T_{remain} \leftarrow T^P$;
**while** $T_{remain} \neq \{\}$ **do**
    $T_{cur} \leftarrow \{\}$;
    **for** *every diagnosis code* $t \in T_{remain}$ **do**
        Create a chunk $C_{test}$ by projecting to $T_{cur} \cup \{t\}$ ;
        **if** $C_{test}$ *is* $k^m$*-anonymous* **then**
            $T_{cur} \leftarrow T_{cur} \cup \{t\}$;
            keep track of the constraint in which $t$ is contained (if any);
    **for** *every diagnosis code* $t \in T_{cur}$ **do**
        **if** $t$ *belongs to a constraint* $u$*, which is different from the constraint of the first diagnosis code added to* $T_{cur}$ **and** *not all diagnosis codes of* $u$ *are added to* $T_{cur}$ **then**
            $T_{cur} \leftarrow T_{cur} - \{t\}$;
    $i \leftarrow i + 1$ ;
    $T_i \leftarrow T_{cur}$;
    $T_{remain} \leftarrow T_{remain} - T_{cur}$;
Create record chunks $C_1, \ldots, C_v$ by projecting to $T_1, \ldots, T_v$;
Create item chunk $C_T$ using $T_T$;
**return** $\{C_1, \ldots, C_v, C_T\}$

Figure 9: VERPART algorithm.

The pseudocode of VERPART is provided in Fig. 9. This algorithm takes as input a cluster $P$, along with the parameters $k$ and $m$, and returns a set of $k^m$-anonymous record chunks $C_1, \ldots, C_v$, and the item chunk $C_T$ of $P$. Given the

set of diagnosis codes $T^P$ in $P$, VERPART computes the support $s(t)$ of every code $t$ in $P$ and moves all diagnosis codes having lower support than $k$ from $T^P$ to a set $T_T$ (lines 2-4). As the remaining codes have support at least $k$, they will participate in some record chunk. Next, it orders $T^P$ according to: (i) $s(t)$, and (ii) the participation of the codes in utility constraints (line 5). Specifically, the diagnosis codes in $P$ that belong to the same constraint $u$ in $U$ form groups, which are ordered two times; first in decreasing $s(t)$, and then in decreasing $s(t)$ of their first (most frequent) diagnosis code.

Subsequently, VERPART computes the sets $T_1, \ldots, T_v$ (lines 6-20). To this end, the set $T_{remain}$, which contains the ordered, non-assigned codes, and the set $T_{cur}$, which contains the codes that will be assigned to the current set, are used. To compute $T_i$ ($1 \leq i \leq v$), VERPART considers all diagnosis codes in $T_{remain}$ and inserts a code $t$ into $T_{cur}$, only if the $C_{test}$ chunk, constructed from $T_{cur} \cup \{t\}$, remains $k^m$-anonymous (line 13). Note that the first execution of the for loop in line 10, will always add $t$ into $T_{cur}$, since $C_{test} = \{t\}$ is $k^m$-anonymous. If the insertion of $t$ to $T_{cur}$ does not render $T_{cur} \cup \{t\}$ $k^m$-anonymous, $t$ is skipped and the algorithm considers the next code. While assigning codes from $T_{remain}$ to $T_{cur}$, VERPART also tracks the utility constraint that each code is contained in (line 14). Next, VERPART iterates over each code $t$ in $T_{cur}$ and removes it from $T_{cur}$, if two conditions are met: (i) $t$ is contained in a utility constraint $u$ that is different from the constraint of the first code assigned to $T_{cur}$, and (ii) all codes in $u$ have also been assigned to $T_{cur}$ (lines 16-17). Removing $t$ enables the algorithm to insert the code into another record chunk (along with the remaining codes of $u$) in a subsequent step. After that, VERPART assigns $T_{cur}$ to $T_i$, removes the diagnosis codes of $T_{cur}$ from $T_{remain}$, and continues to the next set $T_{i+1}$ (lines 18-20).

Last, the algorithm constructs and returns the set $\{C_1, \ldots, C_v, C_T\}$ (lines 21-23). This set consists of the record chunks $C_1, \ldots, C_v$, and the item chunk $C_T$, which are created in lines 21 and 22, respectively.

**Refining.** This operation focuses on further improving the utility of the disassociated dataset, while maintaining Guarantee 1. To this end, we examine the diagnosis codes that reside in the item chunk of each cluster. Consider, for example, Fig. 4. The item chunk of the cluster $P_1$ contains the diagnosis codes 834.0 and 944.01, because the support of these codes in $P_1$ is 2 (i.e., lower than $k = 3$). For similar reasons, these diagnosis codes are also contained in the item chunk of $P_2$. However, the support of these codes in both clusters $P_1$ and $P_2$ is not small enough to violate privacy (i.e., the combination of 834.0 and 944.01 appears as many times as the one of 296.03 and 294.10 which is in the record chunk of $P_2$).

To handle such situations, we introduce the notion of *joint clusters* by allowing different clusters to have common record chunks. Given a set $T^s$ of *refining codes* (e.g., 834.0 and 944.01 in the aforementioned example), which commonly appear in the item chunks of two or more clusters (e.g., $P_1$ and $P_2$), we can define a joint cluster by (i) constructing one or more *shared chunks* after projecting the original records of the initial clusters to $T^s$ and (ii) removing all diagnosis codes in $T^s$ from the item chunks of the initial clusters. Fig. 10 shows a joint cluster, created by combining the clusters $P_1$ and $P_2$ of Fig. 4, when $T^s$={834.0, 944.01}.

Furthermore, large joint clusters can be built by combining smaller joint clusters. Note that the creation of shared chunks is performed similarly to the method of [53], but shared chunks are created by our VERPART algorithm, which also takes into account the utility constraints.

We now provide an analysis of the time complexity of our algorithm.

| Record | | Item | Shared |
|---|---|---|---|
| $P_1$ cluster | | | |
| {296.00, 296.01, 296.02} | | | {834.0,944.01} |
| {296.00, 296.01, 296.02} | {692.71, 695.10} | 401.0 | {944.01} |
| {296.00, 296.02} | {692.71, 695.10} | | {834.0} |
| {296.00, 296.01} | {692.71} | | |
| {296.00, 296.01, 296.02} | {692.71, 695.10} | | |
| $P_2$ cluster | | | |
| {296.03, 295.04} | | | |
| {294.10, 296.03} | | 404.00, | {834.0,944.01} |
| {294.10, 295.04, 296.03} | | 480.1 | |
| {294.10, 295.04} | | | |
| {294.10, 295.04, 296.03} | | | {834.0,944.01} |

Figure 10: Disassociation with a shared chunk.

**Time Complexity.** We first consider each operation of DISASSOCIATION separately. The worst-case time complexity of the horizontal partitioning operation is $O(|D|^2)$. This is because HORPART works similarly to the Quicksort algorithm, but instead of a pivot, it splits each partition by the selecting the code a. Thus, in the worst case, HORPART performs $|D|$ splits and at each of them it re-orders $|D|$ records. The time complexity of vertical partitioning depends on the domain $T^P$ of the input cluster $P$, and not on the characteristics of the complete dataset. The most expensive operation of VERPART is to ensure that a chunk is $k^m$-anonymous, which requires examining $\binom{|T^P|}{m}$ combinations of diagnosis codes. Thus, VERPART takes $O(|T^P|!)$ time, where $T^P$ is small in practice, as we regulate the size of the clusters. Last, the complexity of the refining operation is $O(|D|^2)$. This is because, in the worst case, the number of passes over the clusters equals the number of the clusters in $D$. Thus, the behavior of DISASSOCIATION is dominated by that of HORPART, as the dataset size grows. Note that this analysis refers to a worst-case and that, in practice, our algorithm is as efficient as the method in [53]. This demonstrates that, taking into account utility constraints, has minimal runtime overhead.

## 5. Example of disassociation

This section presents a concrete example of applying DISASSOCIATION to the dataset $D$ of Fig. 1. The input parameters are $k = 3$ and $m = 2$, and that the $maxClusterSize$ parameter of HORPART is set to 6 [3].

**Horizontal partitioning.** First, DISASSOCIATION performs the horizontal partitioning operation on the original dataset $D$, using the HORPART algorithm. The latter algorithm selects 296.00, which participates in constraint $u_1$ of Fig. 3b and has the largest support. It then splits $D$ into two parts, $D_1$ and $D_2$. $D_1$ consists of the records containing 296.00 (i.e., $r_1$-$r_5$), whereas $D_2$ contains the remaining records $r_6$-$r_{10}$. At this point, 296.00 is moved from the domain $T$ of $D_1$ into the set $ignore$, so that it will not be used in subsequent splits of $D_1$. Moreover, the next call of HORPART for $D_1$ (line 13) is performed with the utility constraint $u_1$ as input. Thus, HORPART tries to further partition $D_1$, using the codes of this constraint. On the contrary, an empty $ignore$ set and no utility constraint are given as input to HORPART, when it is applied to $D_2$. As the size of both $D_1$ and $D_2$ is lower than $maxClusterSize$ (condition in line 2 of 8), HORPART produces the dataset in Fig. 11. This dataset is comprised of the clusters $P_1$ and $P_2$, which amount to $D_1$ and $D_2$, respectively.

**Vertical partitioning.** Then, DISASSOCIATION performs vertical partitioning operation, by applying VERPART to each of the clusters $P_1$ and $P_2$. The latter algorithm computes the support of each code in $P_1$, and then moves 401.0, 834.0 and 944.01, from the cluster domain $T_P$ into the set $T_T$ (line 4 in VERPART).

[3] This parameter could be set to any value at least equal to the value of $k$. However, it is fixed to $2{\cdot}k$, because we have observed that this leads to producing good clusters.

| ID | Records |
|---|---|
| $r_1$ | {296.00, 296.01, 296.02, 834.0, 944.01} |
| $r_2$ | {296.00, 296.02, 296.01, 401.0, 944.01, 692.71, 695.10} |
| $r_3$ | {296.00, 296.02, 692.71, 834.0, 695.10} |
| $r_4$ | {296.00, 296.01, 692.71, 401.0} |
| $r_5$ | {296.00, 296.01, 296.02, 692.71, 695.10} |

| ID | Records |
|---|---|
| $r_6$ | {296.03, 295.04, 404.00, 480.1} |
| $r_7$ | {294.10, 296.03, 834.0, 944.01} |
| $r_8$ | {294.10, 295.04, 296.03, 480.1} |
| $r_9$ | {294.10, 295.04, 404.00} |
| $r_{10}$ | {294.10, 295.04, 296.03, 834.0, 944.01} |

Figure 11: Output of horizontal partitioning on $D$.

The codes are moved to $T_T$, which corresponds to the domain of the item chunk, because they have a lower support than $k = 3$. Thus, $T_P$ now contains {296.00, 296.01, 296.02, 692.71, 695.10}, and it is sorted according to the support of these codes in $P_1$ and their participation in a utility constraint of $U$. Specifically, for the utility constraints of Fig. 3b, we distinguish two groups of codes in $T_P$; a group {296.00, 296.01, 296.02}, which contains the codes in $u_1$, and another group {692.71, 695.10} with the codes in $u_2$. Next, VERPART sorts the first group in descending order of the support of its codes. Thus, 296.00 is placed first and followed by 296.01 and 296.02. The second group is sorted similarly. After that, the two groups are sorted in descending order of the support of their first code. Thus, the final ordering of $T_P$ is {296.00, 296.01, 296.02, 692.71, 695.10}.

Subsequently, VERPART constructs the record chunks of $P_1$ (lines 10-14), as follows. First, it selects 296.00 and checks whether the set of projections of the records $r_1$-$r_5$ on this code is $3^2$-anonymous. This holds, as 296.00 appears in all records of $P_1$. Thus, VERPART places 296.00 into the set $T_{cur}$, which will later be used to define the record chunk $C_1$. Then, the algorithm selects 296.01 and checks whether the projections of all records $r_1$-$r_5$ on {296.00, 296.01} are also $3^2$-anonymous. As this is true, 296.01 is moved to $T_{cur}$, and the same procedure

is performed, for each of the codes 296.02, 692.71, and 695.10. When the projections of the records $r_1$-$r_5$ are found to be $3^2$-anonymous, the corresponding code is added to $T_{cur}$. Otherwise, it is left in a set $T_{remain}$ to be used in a subsequent step. Notice that 296.02 and 692.71 are added into $T_{cur}$, but the code 695.10 is not. This is because the combination of codes 296.01 and 695.10 appears in only two records of $P_1$ (i.e., $r_2$ and $r_5$), hence, the projections of records $r_1$-$r_5$ on {296.00, 296.01, 296.02, 692.71, 695.10} are not $3^2$-anonymous.

After considering all codes in $T_P$, VERPART checks whether the codes of a constraint $u \in U$ are only partially added to $T_{cur}$. This is true for 692.71, which is separated from 695.10 of the same constraint $u_2$. Hence, 692.71 is moved from $T_{cur}$ back to $T_{remain}$ (line 17), so that it can be added to the chunk $C_2$ of $P_1$ along with 695.10. After that, the algorithm finalizes the chunk $C_1$, according to $T_{cur}$, empties the latter set, and proceeds to creating $C_2$. By following this procedure for the cluster $P_2$, VERPART constructs the dataset $D^A$ in Fig. 4.

**Refining.** During this operation, DISASSOCIATION constructs the shared chunks, which are shown in Figure 10, as follows. It inspects the item chunks of $P_1$ and $P_2$ in Fig. 4, and it identifies that each of the codes 834.0 and 944.01 appears in two records of $P_1$, as well as in two records of $P_2$. Note that the actual supports of codes in item chunks are available to the algorithm after the vertical partitioning operation, although they are not evident from Fig. 4 (because they are completely hidden in the published dataset). Since the total support of 834.0 and 944.01 in both clusters is $2 + 2 = 4 > k = 3$, the algorithm reconstructs the projections of $r_1$-$r_5$ and $r_6$-$r_{10}$ on the item chunk domain of $P_1$ and $P_2$ respectively, and calls VERPART, which creates the shared chunk of Fig. 10.

## 6. Experimental evaluation

### *6.1. Experimental data and setup*

We implemented all algorithms in C++ and applied them to the *INFORMS* dataset [8], whose characteristics are shown in Table 1. This dataset was used in INFORMS 2008 Data Mining contest, whose objective was to develop predictive methods for identifying high-risk patients, admitted for elective surgery. In our experiments, we retained the diagnosis code part of patient records only.

We evaluated the effectiveness of our DISASSOCIATION algorithm, referred to as *Dis*, by comparing to *CBA*, the state-of-the-art generalization-based algorithm for preventing identity disclosure based on diagnosis codes. The default parameters were $k$=5 and $m$=2, and the hierarchies used in *CBA* were created as in [34]. All experiments ran on an Intel Xeon at 2.4 GHz with 12 GB of RAM.

| **Dataset** | $\|D\|$ | Distinct codes | **Max, Avg # codes/record** |
|---|---|---|---|
| *INFORMS* | 58302 | 631 | 43, 5.11 |

Table 1: Description of the dataset.

To evaluate data utility, we employed the ARE and MRE measures, discussed in Section 3.3. For the computation of ARE, we used two different types of query workloads. The first workload type, referred to as $\mathcal{W}_1$, contains queries asking for sets of diagnosis codes that a certain percentage of all patients have. In other words, these queries retrieve *frequent itemsets* (i.e., sets of diagnosis codes that appear in at least a specified percentage of transactions, expressed using a *minimum support threshold*). Answering such queries accurately is crucial in various biomedical data analysis applications [34], since frequent itemsets serve as building blocks in several data mining models [31]. The second workload type we considered is referred to as $\mathcal{W}_2$ and contains 1000 queries, which retrieve sets of

diagnosis codes, selected uniformly at random. These queries are important, because it may be difficult for data owners to predict many of the analytic tasks that will be applied to anonymized data by data recipients.

In addition, we evaluated MRE using three classes of utility policies: *hierarchy-based*, *similarity-based*, and *frequency-based*. The first two types of policies have been introduced in [34] and model semantic relationships between diagnosis codes. For hierarchy-based policies, these relationships are formed using the ICD hierarchy. Specifically, hierarchy-based utility policies are constructed by forming a different utility constraint for all 5-digit ICD codes that have a common ancestor (other than the root) in the ICD hierarchy. The common ancestor of these codes is a 3-digit ICD code, *Section*, or *Chapter*[4], for the case of *level* 1, *level* 2, and *level* 3 hierarchy-based policies, respectively. The similarity-based utility policies are comprised from utility constraints that contain the same number of sibling 5-digit ICD codes in the hierarchy. Specifically, we considered similarity-based constraints containing 5, 10, 25, and 100 codes and refer to their associated utility policies as *sim* 5, 10, 25, and 100, respectively. Last, we considered frequency-based utility policies that model *frequent itemsets*. We mined frequent itemsets using the *FP-Growth* algorithm [27], which was configured with a varying minimum support threshold in $\{0.625, 1.25, 2.5, 5\}$. Thus, the generated utility constraints contain sets of diagnosis codes that appear in at least $0.625\%$, $1.25\%$, $2.5\%$, and $5\%$ percent of transactions, respectively. The utility policies associated with such constraints are denoted with *sup* 0.625, 1.25, 2.5, and 5, respectively. Unless otherwise stated, we use *level 1*, *sim 10*, and *sup 0.625*, as the

[4]Sections and Chapters are internal nodes in the ICD hierarchy, which model aggregate concepts http://www.cdc.gov/nchs/data/icd9/icdguide10.pdf.

default hierarchy, similarity, and frequency based utility policy, respectively.

### *6.2. Feasibility of identity disclosure*

The risk of performing identity disclosure was quantified by measuring the number of records that share a set (combination) of $m$ diagnosis codes. This number is equal to the inverse of the probability of performing identity disclosure using any subset of these codes. The result in Fig. 12 shows that more than $17\%$ of all sets of 2 diagnosis codes appear in one record. Consequently, more than $17\%$ of patients are uniquely re-identifiable, based on these sets of codes, if the dataset is released intact. Furthermore, fewer than $5\%$ of records contain a diagnosis code that appears at least 5 times. Thus, approximately $95\%$ of records are unsafe, as the corresponding patients are identifiable with probability that exceeds $0.2$, the threshold typically used in privacy-preserving medical data publishing [19]. Moreover, observe that the number of times a set of diagnosis codes appears in the dataset increases with $m$. For example, $96\%$ of sets containing 5 diagnosis codes appear only once. As we will see shortly, our algorithm can guard against attackers with such knowledge, by enforcing $k^m$-anonymity with $m = 5$, and at the same time preserve data utility. This is in contrast to *CBA* and most generalization-based methods (e.g., [54]).

### *6.3. Comparison with* CBA

In this set of experiments, we demonstrate that our method can enforce $k^m$-anonymity, while allowing more accurate query answering than *CBA*.

We first report ARE for query workloads of type $\mathcal{W}_2$ and for the following utility policies: *level* 1 (hierarchy-based), *sim* 10 (similarity-based), and *sup* 1.25 (frequency-based). For a fair comparison, the diagnosis codes retrieved by all

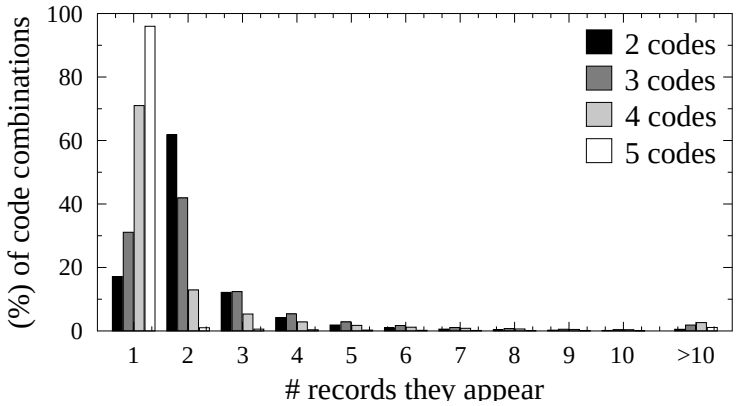


Figure 12: Number of records in which a percentage of combinations, containing 2 to 5 diagnosis codes, appears.

queries are among those that are not suppressed by *CBA*. Fig. 13a illustrates the results for the *level* 1 policy. The ARE for *Dis* is 6 times smaller on average, and up to 16 times smaller, than that of *CBA*. This shows that the use of disassociation instead of generalization allows enforcing $k^m$-anonymity with low information loss. Figs. 13b and 13c show the corresponding results for the similarity-based and frequency-based policies, respectively. Again, our method outperformed *CBA*, achieving ARE scores that are 4.5 and 7.4 times better, on average. Quantitatively similar results were obtained for query workloads of type $\mathcal{W}_1$ (omitted, for brevity).

Next, we report the number of distinct diagnosis codes that are suppressed when $k$ is set to 5, $m$ varies in $[2, 3]$, and the utility policies of the previous experiment are used. The results in Fig. 14 show that *CBA* suppressed a relatively large number of diagnosis codes, particularly when strong privacy is required and the utility constraints are stringent. For instance, $23.6\%$ (i.e., 149 out of 631) of distinct diagnoses codes were suppressed, when $m = 3$ and the *level* 1 utility policy was used. On the contrary, our method released all diagnoses codes intact, as it

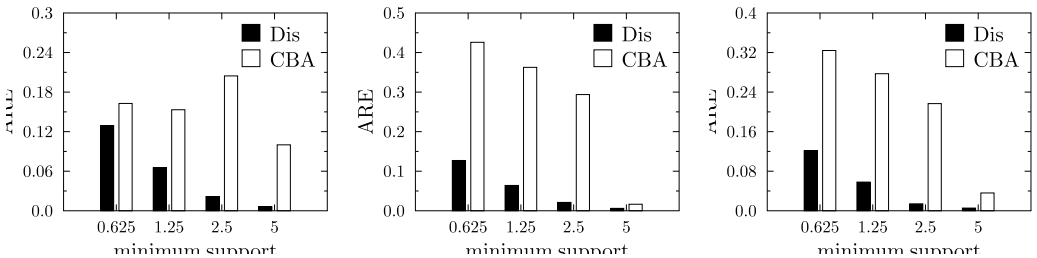


(a) *level* 1 (b) *sim* 10 (c) *sup* 1.25

Figure 13: Comparison with *CBA* with respect to ARE for query workloads of type $\mathcal{W}_2$ and for different utility policies.

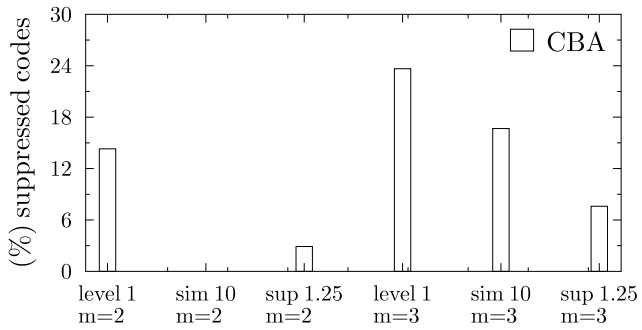


Figure 14: Percentage of distinct diagnosis codes that are suppressed by *CBA* (no diagnosis codes are suppressed by our method, by design).

does not employ suppression. This is particularly useful for medical studies (e.g., in epidemiology), where a large number of codes are of interest.

Having established that our method outperforms *CBA* in terms of achieving $k^m$-anonymity with low information loss, we do not include results for *CBA* in the remainder of the section.

### *6.4. Supporting clinical case count studies*

In the following, we demonstrate the effectiveness of our method at producing data that support clinical case count studies.

Fig. 15a illustrates the results for all three hierarchy-based policies and for

query workloads of type $\mathcal{W}_1$. These workloads require retrieving a randomly selected set of $1$ to $4$ diagnosis codes. For consistency, a set of $c$ diagnosis codes is built (extended) by adding a random code to its subset containing $c-1$ codes. Observe that the error in query answering is fairly small and increases with the size of sets of diagnosis codes. This is because larger sets appear in few records and are more difficult to preserve in $k^m$-anonymous data [53]. Furthermore, it can be seen that low ARE scores are achieved, even for the *level 1* utility policy, which is difficult to satisfy using generalization (e.g., *CBA* suppressed $14.3\%$ of distinct diagnosis codes to satisfy this policy when $m = 2$, as shown in Fig. 14). Similar observations can be made from Figs. 15b and 15c, which show the results for similarity-based and frequency-based constraints, respectively.

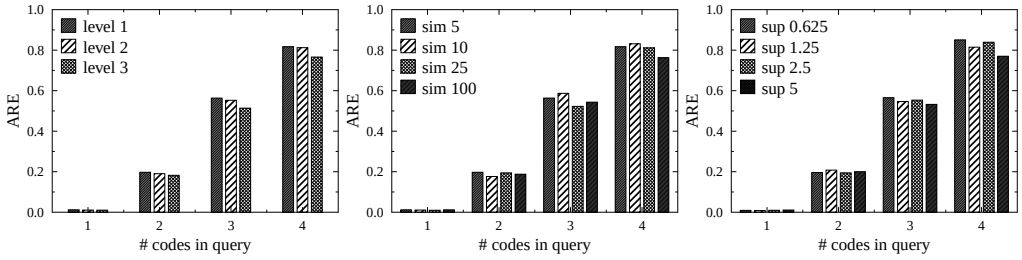


(a) hierarchy-based (b) similarity-based (c) frequency-based

Figure 15: ARE for query workloads of type $\mathcal{W}_1$ that retrieve $1$ to $4$ diagnosis codes and for different utility policies.

Fig. 16a shows the results with respect to ARE, for hierarchy-based constraints and query workloads of type $\mathcal{W}_2$. The corresponding results for similarity-based and frequency-based constraints are reported in Figs. 16b and 16c, respectively. Note that ARE scores are very low, in all tested cases. In addition, queries involving more frequent sets of diagnosis codes (i.e., sets mined with a higher minimum support threshold) can be answered highly accurately, which helps pre-

serve data utility in various data mining tasks.

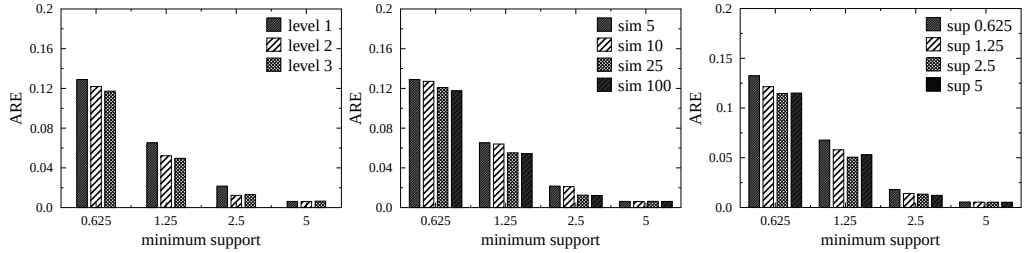


(a) hierarchy-based (b) similarity-based (c) frequency-based

Figure 16: ARE for query workloads of type $\mathcal{W}_2$ and for different utility policies.

Next, we examined the impact of $k$ on ARE by varying this parameter in $[5, 25]$, setting $m$ to 2, and considering the *level 1*, *sim* 10, and *sup* 2.5 utility policies. The results, reported in Fig. 17, show that ARE increases with $k$. This is because it is more difficult to retain associations between diagnosis codes, when clusters are large. However, the ARE scores are low (i.e., no more than $0.05$), which confirms that our method permits accurate query answering, even for large $k$ values that offer more privacy.

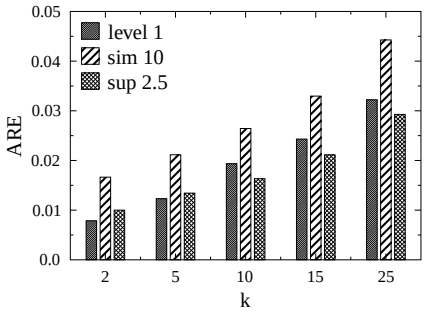


Figure 17: ARE for varying $k$ in $[5, 25]$ and for different utility policies.

### *6.5. Effectiveness in medical analytic tasks*

In this set of experiments, we evaluate our method in terms of its effectiveness at supporting different utility policies. Given a utility policy, we measure MRE,

for all constraints in the policy, and report the percentage of constraints, whose MRE falls into a certain interval. Recall from Section 6.1 that intervals whose endpoints are close to zero are preferred.

Fig. 18 reports the results with respect to MRE for the *level 1* utility policy. As can be seen, the MRE of all constraints in this policy is in $[-24\%, 5\%)$, while the MRE of the vast majority of constraints falls into much narrower intervals. For instance, $81\%$ and $90\%$ of these constraints have an MRE in $[-2.5\%, 2.5\%)$ and in $[-5\%, 5\%)$, respectively. Furthermore, the percentage of constraints with an MRE score close to zero is generally higher compared to those with MRE is far from zero. For example, $37.6\%$ of the constraints have MRE in $[-2.5\%, 0\%]$, whereas only $3.7\%$ of them have an MRE in $[-24\%, -10\%)$. This confirms that the data produced by our method can support the intended analytic tasks, in addition to permitting accurate query answering.

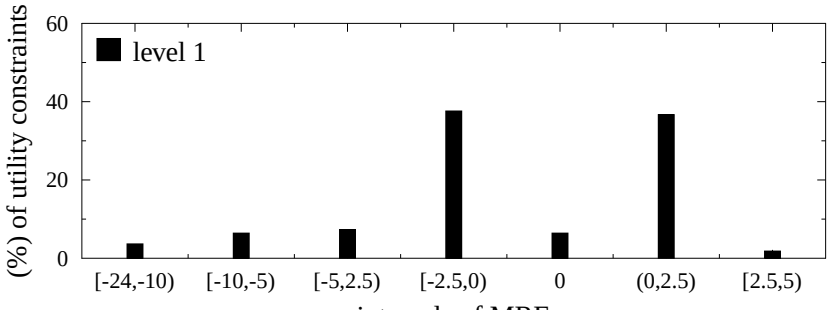


Figure 18: MRE for *level 1* utility policy.

Next, we performed a similar experiment for similarity-based and frequency-based utility policies. The results for the *sim 5* policy are shown in Fig. 19. Note that $81\%$ and $90\%$ of the utility constraints in this policy have an MRE in $[-2.5\%, 2.5\%]$ and in $[-5\%, 5\%)$, respectively and only $3.6\%$ of them have an MRE in $[-21\%, -10\%)$. The results for the *sup 0.625* utility policy are quantita-

tively similar, as can be seen in Fig. 20. That is, all constraints in this policy have an MRE in a narrow range $[-10\%, 5\%)$. These results together with those in Figs. 18 and 19 suggest that the data produced by our method can support different types of utility policies fairly well.

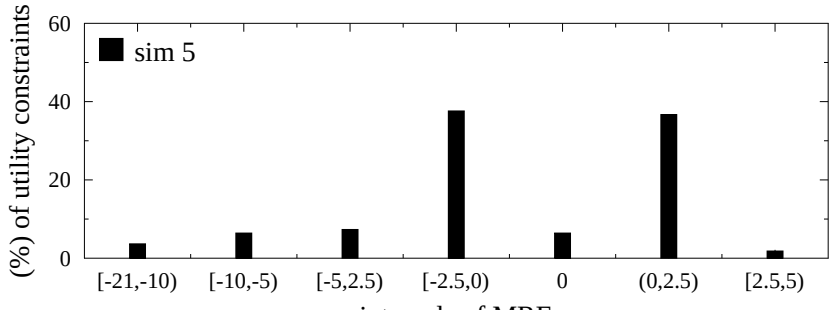


Figure 19: MRE for the *sim 5* utility policy.

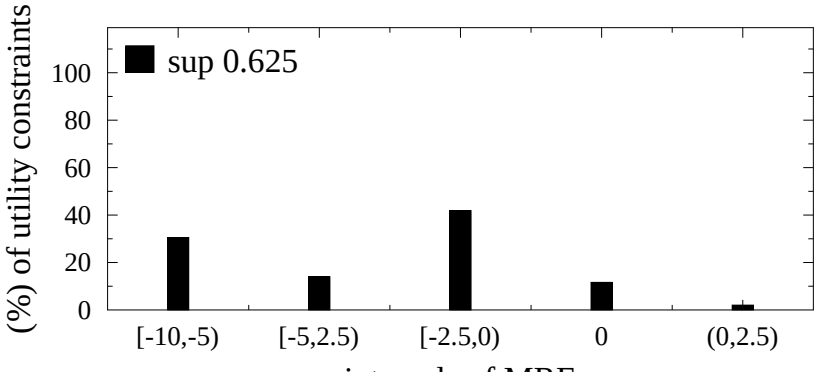


Figure 20: MRE for the *sup 0.625* utility policy.

In addition, we examined the impact of $k$ on MRE, for different classes of utility policies. Figs. 21, 22, and 23 illustrate the results for hierarchy-based, similarity-based, and frequency-based policies, respectively. It can be seen that, lowering $k$, helps the production of data that support the specified utility policies. For instance, $95.3\%$ of hierarchy-based constraints have an MRE in $[-5\%, 5\%)$

when $k = 2$, but $53\%$ of such constraints have an MRE in this interval when $k = 25$. The corresponding percentages are $100\%$ and $33\%$ for similarity-based utility constraints, and $95\%$ and $59\%$ for frequency-based utility constraints. This is expected due to the utility/privacy trade-off. However, the MRE of most of the constraints (i.e., $75.7$, $72.3$, and $85.9\%$ on average, for the tested $k$ values, in the case of hierarchy-based, similarity-based, and frequency-based constraints) falls into $[-5\%, 5\%)$. Thus, our method is effective at supporting the intended medical analytic tasks.

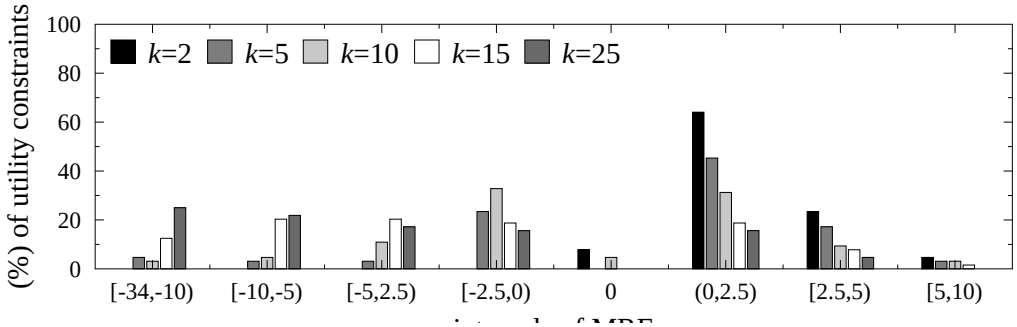


Figure 21: MRE for hierarchy-based utility policies and for varying $k$ in $[2, 25]$.

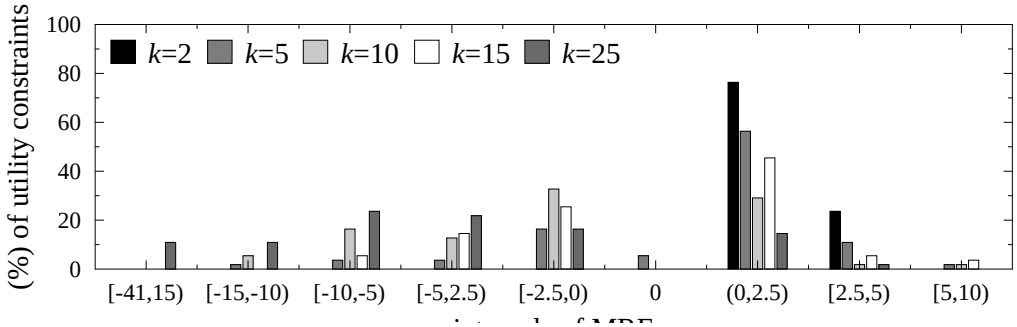


Figure 22: MRE for similarity-based utility policies and for varying $k$ in $[2, 25]$.

Last, we investigated the effectiveness of our method with respect to MRE, when $m$ is set to $5$. It is interesting to examine data utility in this setting, because

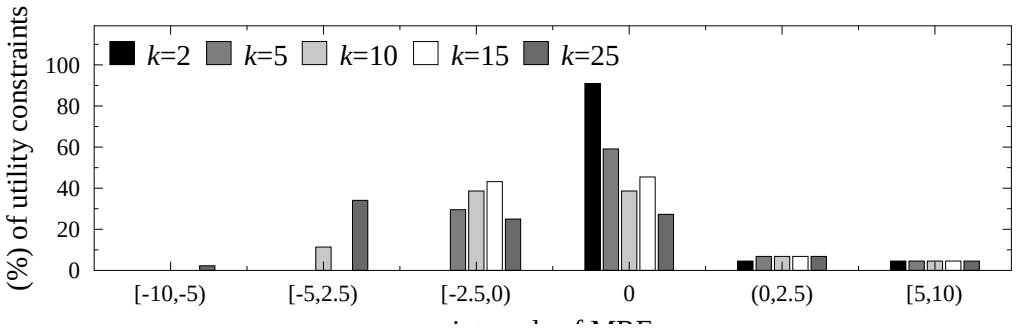


Figure 23: MRE for frequency-based utility policies and for varying $k$ in $[2, 25]$.

a patient's record in discharge summaries, which may be used in identity disclosure attacks, often contains $5$ diagnosis codes, which are assigned during a single hospital visit. Thus, enforcing $k^m$-anonymity, using $m = 5$, provides protection from such attacks, assuming a worst case scenario in which data owners do not know which diagnoses codes may be used by attackers. In our experiments, we considered different classes of utility policies (namely, *level* 1, *sim* 10, and *sup* 2.5) and report the results in Fig. 24. Notice that the data produced by our method remain useful for supporting the utility policies, as $89\%$, $93\%$, and $100\%$ of the tested hierarchy-based, similarity-based, and frequency-based constraints have an MRE in $[-5\%, 5\%)$, respectively.

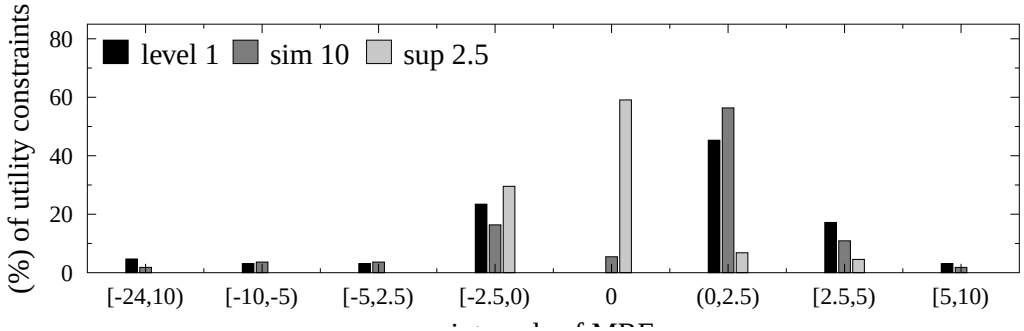


Figure 24: MRE for different types of utility policies and for $m = 5$.

## 7. Discussion

This section explains how our approach can be extended to deal with different types of medical data and privacy requirements.

### *7.1. Dealing with data of different types*

Our work considers records comprised of a set of diagnosis codes, following [33, 35, 34]. However, some applications require different types of data. For example, applications that aim at identifying phenotypes in the context of genetic association studies, require data in which a record contains repeated diagnosis codes (i.e., a multiset of diagnosis codes). Dealing with these applications is straightforward, as it requires a pre-processing in which different instances of the same diagnosis code in the dataset, and the utility constraints, are mapped to different values (e.g., the first occurrence of 250.01 is mapped to 250.011, the second to 250.012 etc.) [34]. Other applications require releasing data that contains both diagnosis codes and demographics. Anonymizing this type of data has been considered very recently [48], although the proposed methodology employs generalization and is not directly applicable to releasing patient information. Extending our approach, so that it can be used as a component of this methodology is an interesting direction for future work.

### *7.2. Dealing with different privacy requirements*

Our work focuses on preventing *identity disclosure* which is the most important privacy requirement in the healthcare domain. It ensures that an attacker with background knowledge of up to $m$ codes in a record cannot associate this record with fewer than $k$ candidate patients. However, the anonymization framework we propose is not restricted to guarding against attackers with only partial knowledge

of the codes in a record in $D$. In fact, by setting $m$ to the maximum number of codes in a record of $D$, data owners can prevent attacks based on knowledge of all codes in a record. This is because the dataset that is produced by our method in this case satisfies Guarantee 1. Regardless of the specific values of $k$ and $m$, we do not consider collaborative attacks, where two or more attackers combine their knowledge in order to re-identify a patient nor attackers with background knowledge of multiple records in $D$. Such powerful attack schemes can only be handled within stronger privacy principles, such as differential privacy (see Section 2). However, applying these principles usually results in significantly lower utility, compared to the output of our method, which offers a reasonable tradeoff.

Furthermore, we do not assume any distinction between sensitive and non-sensitive diagnosis codes (see Section 3). Instead, we treat all codes as potentially identifying. However, when there is clear distinction between sensitive and non-sensitive codes in a record, i.e., data owners know that some codes (the sensitive ones) are not known to any attacker, then our framework allows thwarting *attribute disclosure* as well. An effective principle for preventing attribute disclosure is $\ell$-diversity [40]. Enforcing $\ell$-diversity using our framework is rather straightforward, as it simply requires (i) ignoring all sensitive codes during the horizontal partitioning operation, and (ii) placing all sensitive codes in the item chunk during vertical partitioning. This produces a dataset $D^A$, in which all sensitive codes are contained in the item chunks. This dataset limits the probability of any association between sensitive codes and any other subrecord or code to $\frac{1}{|P|}$, where $|P|$ is the size of the cluster. Clearly, the desired degree of $\ell$-diversity can be achieved in this case, by adjusting the size of the clusters.

In general, protection from attribute disclosure within our framework tends

to incur higher information loss than simply protecting from identity disclosure. This is because sensitive codes are not necessarily infrequent, i.e., they may appear more than $k$ times in a cluster. Thus, the frequent sensitive codes that would be placed in a $k^m$-anonymous record chunk, when only identity disclosure is prevented, are now placed in the item chunk and each of them is completely disassociated from any other. In this case, the utility constraints that include sensitive codes are not preserved in the published dataset to the extent they would be preserved when only guarding against identity disclosure is required. Of course, this does not hold for the remaining utility constraints. The evaluation of our method with protection from both identity and attribute disclosure is left as future work.

## 8. Conclusions

Ensuring that diagnosis codes cannot be used in identity disclosure attacks is necessary but challenging, particularly when data need to be shared broadly and to support a range of medical analytic tasks that may not be determined prior to data dissemination. To this end, we proposed a novel, disassociation-based approach that enforces $k^m$-anonymity with low information loss. Our approach does not require data owners to specify diagnosis codes, as existing methods do, and takes into account analytic tasks that published data are intended for. Extensive experiments using EHR data confirm that our approach can produce data that permit various types of clinical case count studies and general medical analysis tasks to be performed accurately.

[1] National Institutes of Health. Policy for sharing of data obtained in NIH supported or conducted genome-wide association studies. NOT-OD-07-088. 2007.

[2] The Clinical Practice Research Datalink. http://www.cprd.com/.

[3] EU Directive 95/46/EC of the European Parliament and of the Council. http://eur-lex.europa.eu/LexUriServ/LexUriServ.do?uri=CELEX:31995L0046:en:HTML.

[4] Health data initiative. Institute of Medicine and the U.S. Department of Health and Human Services (HHS). http://www.hhs.gov/open/initiatives/hdi/.

[5] The Secure Anonymised Information Linkage (SAIL) Databank. http://www.ehi2.swansea.ac.uk/en/sail-databank.htm.

[6] UK Anonymization Code. Information Commissioner's Office. http://www.ico.org.uk/for_organisations/data_protection/topic_guides/anonymisation/.

[7] Widening the use of Electronic Health Record data for research. National Center for Research Resources (US), 2009. http://videocast.nih.gov/summary.asp?live=8062.

[8] INFORMS Data Mining Contest, 2008. https://sites.google.com/site/informsdataminingcontest/.

[9] R. V. Atreya, J. C. Smith, A. B. McCoy, B. Malin, and R. A. Miller. Reducing patient re-identification risk for laboratory results within research datasets. *Journal of the American Medical Informatics Association*, 20(1):95–101, 2013.

[10] M. Canim, M. Kantarcioglu, and B. Malin. Secure management of biomedical data with cryptographic hardware. *IEEE Transactions on Information Technology in Biomedicine*, 16(1):166–175, 2012.

[11] J. Cattell, S. Chilukuri, and M. Levy. How big data can revolutionize pharmaceutical R&D. McKinsey Company, Insights and Publications, 2013. http://www.mckinsey.com/insights/health_systems_and_services.

[12] G. Cormode. Personal privacy vs population privacy: learning to attack anonymization. In *KDD*, pages 1253–1261, 2011.

[13] F. K. Dankar and K. El Emam. The application of differential privacy to health data. In *EDBT/ICDT Workshops*, pages 158–166, 2012.

[14] J.C. Denny. Chapter 13: Mining electronic health records in the genomics era. *PLoS Computational Biology*, 8(12):e1002823, 12 2012.

[15] U.S. Department of Health & Human Services. Breaches affecting 500 or more individuals, 2013. http://www.hhs.gov/ocr/privacy/hipaa/administrative/breachnotificationrule/breachtool.html.

[16] C. Dwork. Differential privacy. In *ICALP*, pages 1–12, 2006.

[17] M. Elliot, K. Purdam, and D. Smith. Statistical disclosure control architectures for patient records in biomedical information systems. *Journal of Biomedical Informatics*, 41(1):58 – 64, 2008.

[18] K. El Emam. Methods for the de-identification of electronic health records. *Genome Medicine*, 3(25), 2010.

[19] K. El Emam and F. K. Dankar. Protecting privacy using k-anonymity. *Journal of the American Medical Informatics Association*, 15(5):627–637, 2008.

[20] K. El Emam, F. Kamal Dankar, R. Issa, E. Jonker, D. Amyot, E. Cogo, J. Corriveau, M. Walker, S. Chowdhury, R. Vaillancourt, T. Roffey, and J. Bottomley. A globally optimal k-anonymity method for the de-identification of health data. *Journal of American Medical Informatics Association*, 16(5):670–682, 2009.

[21] L. Fan, L. Xiong, and V. S. Sunderam. Fast: differentially private real-time aggregate monitor with filtering and adaptive sampling. In *SIGMOD*, pages 1065–1068, 2013.

[22] S. Fienberg, W. Fulp, A. Slavkovic, and T. Wrobel. Secure log-linear and logistic regression analysis of distributed databases. In *Privacy in statistical databases*, pages 277–290, 2006.

[23] B.C.M. Fung, K. Wang, R. Chen, and P.S. Yu. Privacy-preserving data publishing: A survey of recent developments. *ACM Comput. Surv.*, 42(4):14:1–14:53, 2010.

[24] J. J. Gardner, L. Xiong, Y. Xiao, J. Gao, A. R. Post, X. Jiang, and L. Ohno-Machado. Share: system design and case studies for statistical health information release. *Journal of the American Medical Informatics Association*, 20(1):109–116, 2013.

[25] G. Ghinita, Y. Tao, and P. Kalnis. On the anonymization of sparse high-dimensional data. In *ICDE*, pages 715–724, 2008.

[26] A. Gkoulalas-Divanis and G. Loukides. *Anonymization of Electronic Medical Records to Support Clinical Analysis*. Springer, 2013.

[27] J. Han, J. Pei, and Y. Yin. Mining frequent patterns without candidate generation. *SIGMOD Rec.*, 29(2):1–12, May 2000.

[28] Y. He and J. F. Naughton. Anonymization of set-valued data via top-down, local generalization. *Proceedings of the VLDB Endowment*, 2(1):934–945, 2009.

[29] D. Kifer and A. Machanavajjhala. No free lunch in data privacy. In *SIGMOD*, pages 193–204, 2011.

[30] K. LeFevre, D.J. DeWitt, and R. Ramakrishnan. Incognito: efficient full-domain k-anonymity. In *SIGMOD*, pages 49–60, 2005.

[31] K. LeFevre, D.J. DeWitt, and R. Ramakrishnan. Workload-aware anonymization. In *KDD*, pages 277–286, 2006.

[32] N. Li, T. Li, and S. Venkatasubramanian. t-closeness: Privacy beyond k-anonymity and l-diversity. In *ICDE*, pages 106–115, 2007.

[33] G. Loukides, J.C. Denny, and B. Malin. The disclosure of diagnosis codes can breach research participants' privacy. *Journal of the American Medical Informatics Association*, 17:322–327, 2010.

[34] G. Loukides and A. Gkoulalas-Divanis. Utility-aware anonymization of diagnosis codes. *IEEE Journal of Biomedical and Health Informatics*, 17(1):60–70, 2013.

[35] G. Loukides, A. Gkoulalas-Divanis, and B. Malin. Anonymization of electronic medical records for validating genome-wide association studies.

*Procedings of the National Academy of Sciences USA*, 107:7898–7903, 2010.

[36] G. Loukides, A. Gkoulalas-Divanis, and B. Malin. COAT: Constraint-based anonymization of transactions. *Knowledge and Information Systems*, 28(2):251–282, 2011.

[37] G. Loukides, A. Gkoulalas-Divanis, and J. Shao. Anonymizing transaction data to eliminate sensitive inferences. In *DEXA*, pages 400–415, 2010.

[38] G. Loukides, A. Gkoulalas-Divanis, and J. Shao. Efficient and flexible anonymization of transaction data. *Knowledge and Information Systems*, 36(1):153–210, 2013.

[39] G. Loukides and J. Shao. Capturing data usefulness and privacy protection in k-anonymisation. In *SAC*, pages 370–374, 2007.

[40] A. Machanavajjhala, J. Gehrke, D. Kifer, and M. Venkitasubramaniam. l-diversity: Privacy beyond k-anonymity. In *ICDE*, page 24, 2006.

[41] B. Malin and L. Sweeney. How (not) to protect genomic data privacy in a distributed network: using trail re-identification to evaluate and design anonymity protection systems. *Journal of Biomedical Informatics*, 37(3):179 – 192, 2004.

[42] N. Marsden-Haug, V.B. Foster, P.L. Gould, E. Elbert, H. Wang, and J.A. Pavlin. Code-based syndromic surveillance for influenzalike illness by international classification of diseases, ninth revision. *Emerging Infectious Diseases*, 13(2):207–216, 2007.

[43] Sergio MartíNez, David SáNchez, and Aida Valls. A semantic framework to protect the privacy of electronic health records with non-numerical attributes. *Journal of Biomedical Informatics*, 46(2):294–303, 2013.

[44] M. D. Mailman MD, M. Feolo M, and Y. Jin et al. The ncbi dbgap database of genotypes and phenotypes. *Nature Genetics*, 39:1181–6, 2007.

[45] N. Mohammed, R. Chen, B. C. M. Fung, and P. S. Yu. Differentially private data release for data mining. In *KDD*, pages 493–501, 2011.

[46] National Committee on Vital and Health Statistics. HIPAA Code Set Rule. http://www.ncvhs.hhs.gov/091210p06b.pdf.

[47] B. Pinkas. Cryptographic techniques for privacy-preserving data mining. *ACM Special Interest Group on Knowledge Discovery and Data Mining Explorations*, 4(2):12–19, 2002.

[48] G. Poulis, G. Loukides, A. Gkoulalas-Divanis, and S. Skiadopoulos. Anonymizing data with relational and transaction attributes. In *ECML/PKDD (to appear)*.

[49] P. Samarati. Protecting respondents identities in microdata release. *IEEE Transactions on Knowledge and Data Engineering*, 13(9):1010–1027, 2001.

[50] R. S. Sandhu, E. J. Coyne, H. L. Feinstein, and C. E. Youman. Role-based access control models. *IEEE Computer*, 29(2):38–47, 1996.

[51] L. Sweeney. k-anonymity: a model for protecting privacy. *International*

*Journal on Uncertainty, Fuzziness and Knowledge-based Systems*, 10:557–570, 2002.

[52] A. Tamersoy, G. Loukides, J. C. Denny, and B. Malin. Anonymization of administrative billing codes with repeated diagnoses through censoring. In *Proceedings of the 2010 AMIA Anual Symposium*, pages 782–786, 2010.

[53] M. Terrovitis, J. Liagouris, N. Mamoulis, and S. Skiadopoulos. Privacy preservation by disassociation. *Proceedings of the VLDB Endowment*, 5(10):944–955, 2012.

[54] M. Terrovitis, N. Mamoulis, and P. Kalnis. Privacy-preserving anonymization of set-valued data. *Proceedings of the VLDB Endowment*, 1(1):115–125, 2008.

[55] S. Wang, X. Jiang, Y. Wu, L. Cui, S. Cheng, and L. Ohno-Machado. Expectation propagation logistic regression (explorer): Distributed privacy-preserving online model learning. *Journal of Biomedical Informatics*, 46(3):480 – 496, 2013.

[56] X. Xiao and Y. Tao. Personalized privacy preservation. In *SIGMOD*, pages 229–240, 2006.

[57] J. Xu, W. Wang, J. Pei, X. Wang, B. Shi, and A. W-C. Fu. Utility-based anonymization using local recoding. In *KDD*, pages 785–790, 2006.

[58] Y. Xu, K. Wang, A. W-C. Fu, and P. S. Yu. Anonymizing transaction databases for publication. In *KDD*, pages 767–775, 2008.